



Improving Seasonal Arctic Sea Ice Predictions with the Combination of Machine Learning and Earth System Model

Zikang He^{1,2,3}, Yiguo Wang³, Julien Brajard³, Xidong Wang^{1,2}, and Zheqi Shen^{1,2}

¹Key Laboratory of Marine Hazards Forecasting, Ministry of Natural Resources, Hohai University, Nanjing, 210098, China

²College of Oceanography, Hohai University, Nanjing, 210098, China

³Nansen Environmental and Remote Sensing Center, Jahnebakken 3, Bergen, N-5007, Norway

Correspondence: Yiguo Wang (Yiguo.wang@nersc.no) and Xidong Wang (xidong_wang@hhu.edu.cn)

Abstract. While dynamical models are essential for seasonal Arctic sea ice prediction, they often exhibit significant errors that are challenging to correct. In this study, we integrate a multilayer perceptron (MLP) machine learning (ML) model into the Norwegian Climate Prediction Model (NorCPM) to improve seasonal sea ice predictions. We compare the online and offline error correction approaches. In the online approach, ML corrects errors in the model's instantaneous state during the model simulation, while in the offline approach, ML post-processes and calibrates predictions after the model simulation. Our results show that the ML models effectively learn and correct model errors in both methods, leading to improved predictions of Arctic sea ice during test periods (i.e., 2003-2021). Both methods yield the most significant improvements in the marginal ice zone, where error reductions in sea ice concentration exceed 20%. These improvements vary seasonally, with the most substantial enhancements occurring in the Atlantic, Siberian, and Pacific regions from September to January. The offline error correction approach consistently outperforms the online error correction approach. Notably, in September, the online approach reduces the error of the pan-Arctic sea ice extent by 50%, while the offline approach achieves a 75% error reduction.

1 Introduction

According to satellite observations, the Arctic sea ice extent (SIE) rapidly declines throughout all calendar months during the recent decades (e.g., Serreze et al., 2007). The most significant reductions occurred in the summer and autumn (e.g., September, Stroeve et al., 2014). The wider open ocean leads to growing socioeconomic activities in the Arctic (e.g., fisheries, shipping, and resource extraction). These increased human activities highly demand accurate seasonal predictions of Arctic sea ice



conditions (Jung et al., 2016; Wagner et al., 2020). The Sea Ice Outlook, managed by the Sea Ice Prediction Network, produces monthly reports during the Arctic sea ice retreat season. These monthly reports synthesize input from the international research community devoted to enhancing sea ice predictions. Recently, Bushuk et al. (2024) evaluated and compared 17 statistical models, 17 dynamical models, and 1 heuristic approach in predicting September Arctic sea ice. They found that dynamical and statistical models are overall comparable in predicting the Pan-Arctic SIE, and dynamical models generally outperform statistical models in predicting the regional SIE and sea ice concentration (i.e., local quantities). Bushuk et al. (2024) also suggested the dynamical models must further improve their initialization and model resolution to reduce prediction errors.

Data assimilation (DA) integrates observations with dynamical models to optimally estimate the state of the climate system (Carrassi et al., 2018; Penny and Hamill, 2017). It has widespread application in producing reanalysis (Saha et al., 2006; Dee et al., 2011; Zuo et al., 2019; Laloyaux et al., 2018; Hersbach et al., 2020), offering comprehensive, continuous, and dynamically consistent reconstructions of past climate states. Simultaneously, many prediction centers are transitioning to DA adoption to mitigate uncertainties in initial conditions (Kimmritz et al., 2019; Blockley and Peterson, 2018; Wang et al., 2013, 2019; Bushuk et al., 2024; Vitart et al., 2017). The improved density and quality of observations across different climate system components and advanced DA methods enable more precise initial conditions for seasonal predictions of Arctic sea ice. Nevertheless, even with perfect initial conditions, prediction errors escalate over time due to the inherent deficiencies of dynamical models in emulating the true climate system (gray line and pink line in Figure 1). This underscores the necessity for dealing with prediction errors.

Machine learning (ML) has recently emerged as a data-driven technique to mitigate dynamical prediction errors. Two prevalent approaches include constructing an ML-dynamical hybrid model (e.g., Brajard et al., 2021; Watt-Meyer et al., 2021) and post-processing/calibrating model output (e.g. Palermé et al., 2024; Yang et al., 2023). The former is considered as online error correction, while the latter refers to offline error correction.

In the context of online error correction, ML is applied to correct errors in the instantaneous model state (i.e., initial conditions for the following model integration) and sequentially applied to update the instantaneous model state during simulation (e.g., Brajard et al., 2021), referring to an ML-dynamical hybrid model (purple line in Figure 1). Such online error correction approaches have been investigated in both an idealized framework (e.g., Watson, 2019; Brajard et al., 2021) and real applications (e.g., Watt-Meyer et al., 2021).

Watson (2019) examined the tendency error correction approach in the Lorenz 96 model. Brajard et al. (2021) explored the resolvent error correction approach in the two-scale Lorenz model as well as in a low-order coupled ocean-atmosphere model called the Modular Arbitrary-Order Ocean-Atmosphere Model (MAOOAM) (De Cruz et al., 2016). Watt-Meyer et al. (2021) demonstrated that the online error correction can improve the short-term forecasting skills and accuracy of precipitation simulation while the dynamical model can run indefinitely without numerical instabilities arising. Gregory et al. (2024) applied ML to correct sea ice errors in an ocean-ice coupled model and demonstrated that ML can effectively reduce sea ice bias online in a 5-year simulation. So far, the ML-based online error correction method has not been tested for seasonal sea ice prediction in an Earth system model. In this study, we will build and assess a hybrid model combining ML and a state-of-the-art Earth system model for seasonal prediction of Arctic sea ice.



On the other hand, the offline error correction consists in performing post-processing (also called calibration) of the dynamical model predictions (blue line in Figure 1). ML is trained to predict errors for time-averaged model outputs (e.g., daily or monthly outputs) and applied to correct errors present in raw predictions. The most common error correction methods employed in sea ice prediction (Bushuk et al., 2024) are relatively simple (e.g., correction of the mean error or a linear regression adjustment, Blanchard-Wrigglesworth et al., 2017). More recently, Palerm et al. (2024) applied ML to improve the skill of sea ice concentration forecasts on the weather timescale. Overall, they illustrated that ML-based offline calibration reduced the SIC prediction errors by 41% and the ice edge distance error by 44%. Their application is mainly focused on short-term sea ice prediction within 10 days in an ocean-ice coupled model. We will apply and assess the ML-based calibration for seasonal prediction of Arctic sea ice in a state-of-the-art fully-coupled Earth system model.

In this study, we apply ML to the Norwegian Climate Prediction Model (NorCPM, Wang et al., 2019), a fully-coupled Earth system model, for seasonal prediction of Arctic sea ice. We test and compare the ML-based online and offline error correction approaches. In the online approach, we build a hybrid model combining ML and NorCPM to update the instantaneous sea ice state during the production of seasonal predictions. In the offline approach, we use ML to calibrate raw seasonal predictions of Arctic sea ice. The comparison between the two approaches within the same framework delivers new insights for the sea ice prediction community into how to effectively use ML for seasonal Arctic sea ice predictions.

The paper is organized as follows: section 2 presents the model, experimental design, and metrics for validation. Section 3 shows the results of different experiments. We finish with conclusions and discussions in section 4.

2 Methods and data

2.1 Norwegian Climate Prediction Model

The dynamical model we used is NorCPM (Counillon et al., 2014, 2016; Kimmritz et al., 2018, 2019; Wang et al., 2016, 2017). It combines the Norwegian Earth System Model version 1 (NorESM1, Bentsen et al., 2013) and an advanced flow-dependent DA method named ensemble Kalman filter (EnKF, Evensen, 2003).

NorESM1 (Bentsen et al., 2013) is a fully-coupled Earth system model used for climate simulations. Its ocean component is the Bergen Layered Ocean Model (BLOM, Bentsen et al., 2013) – an updated version of the isopycnal coordinate ocean model MICOM (Bleck et al., 1995). The sea ice component is the Los Alamos sea ice model version 4 (CICE4, Gent et al., 2011; Holland et al., 2012). The atmospheric component is a variant of the Community Atmosphere Model version 4 (CAM4-Oslo, Kirkevåg et al., 2018). The land component is the Community Land Model (CLM4, Lawrence et al., 2011; Thornton, 2010). Furthermore, the version 7 coupler (CPL7, Craig et al., 2012) is utilized for inter-component communication and interaction. The external forcings follow the protocol of the Coupled Model Intercomparison Project Phase 5 (CMIP5) historical experiment (Taylor et al., 2012).

The atmospheric and land components are situated on the National Center for Atmospheric Research (NCAR) finite-volume 2° grid, featuring a regular $1.9^\circ \times 2.5^\circ$ latitude–longitude resolution with 26 hybrid sigma–pressure levels extending to 3 hPa. The ocean and sea ice components utilize NCAR’s gx1v6 horizontal grid, which is a nominal 2° resolution curvilinear grid



with the northern pole singularity shifted over Greenland (Bethke et al., 2021). This grid is enhanced both meridionally towards the equator and zonally and meridionally towards the poles. The ocean component comprises 51 isopycnic layers, featuring a bulk mixed layer representation on top with two layers having time-evolving thicknesses and densities.

The sea ice component is equipped with several ice thickness categories (we use the predefined value of $N=5$) to account for the different thermodynamic and dynamic properties of ice with different thicknesses. The volume of snow and ice, energy content, as well as ice concentration, surface temperature, and the volume-weighted mean ice age are determined for each of the ice thickness categories (Bentsen et al., 2013; Kimmritz et al., 2018, 2019).

NorESM1 tends to overly produce thick sea ice, especially in the polar oceans adjacent to the Eurasian continent. This is partly due to factors such as weaker winds across the polar basin and overestimated Arctic cloudiness, which slows little summer snowmelt. Consequently, the summer sea ice extent in the Arctic is too large, contributing to an underestimation of global temperatures (Bentsen et al., 2013; Bethke et al., 2021).

NorCPM uses an EnKF-based anomaly-field DA scheme to update unobserved ocean and sea ice variables by leveraging state-dependent covariance from the simulation ensemble (Kimmritz et al., 2018, 2019). The EnKF allows the assimilation of observations of various types while accounting for observational errors, spatial coverage, and the evolving covariance with the climate state. The EnKF ensures accurate ensemble predictions by representing uncertainties in the initial conditions, propagating these uncertainties over time, and providing a spatiotemporal estimate.

2.2 Data

The reanalysis of NorCPM combining observations with NorESM is a physically consistent construction of the Earth system (Counillon et al., 2016; Kimmritz et al., 2019) and represents the upper limit of the sea ice predictability of NorCPM. In this study, we use the reanalysis as the "truth" to assess the improvement achieved by the error correction methods.

The reanalysis is available from 1980 to 2021 with 30 ensemble members. The initial states of the reanalyses on 15 January 1980 are taken from a NorESM ensemble run integrated from 1850 to 1980 with CMIP5 historical forcings. In this reanalysis, NorCPM assimilates monthly anomalies of sea surface temperature (SST), SIC, and subsurface hydrographic profile data in the middle of each month.

The DA setting slightly differs for two different periods 1980-2002 and 2003-2021. From 1980 to 2002, the climatology used for anomaly assimilation is defined over the period 1980–2010. SST and SIC observations are from HadISST2 (Titchner and Rayner, 2014) and subsurface hydrographic profile data from EN4.2.1 (Good et al., 2013). The assimilation process contains two steps addressed in Kimmritz et al. (2019): firstly, hydrographic DA updates the ocean state (Wang et al., 2017). Subsequently, SST and SIC data assimilation occurs, updating the sea ice and ocean states within the ocean mixed layer. From 2003 to 2021, the climatology utilized for anomaly assimilation is defined from 1982 to 2016. SST and SIC observations are from OISST (Reynolds et al., 2007) and subsurface hydrographic profile data from EN4.2.1 (Good et al., 2013). Strong-coupled DA is performed in a single step to simultaneously update the sea ice and ocean states.

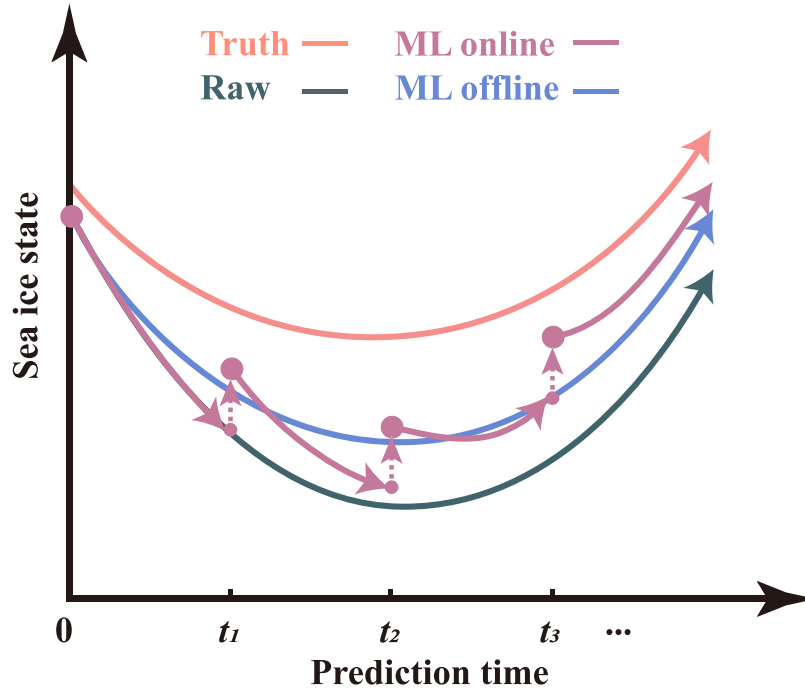


Figure 1. Schema for the online and offline ML-based error correction methods. The pink line represents the truth. The gray line represents dynamical prediction without error correction. The purple (blue) line represents prediction with online (offline) ML-based error correction. The purple dashed arrows indicate pauses during the prediction production, facilitating correction to the instantaneous model state.

2.3 Online error correction approach

The online error correction approach is built from the analysis increment of the reanalysis introduced in section 2.2 (Brajard et al., 2021; Gregory et al., 2024) and sequentially applied to update the instantaneous model state in the middle of each month during prediction simulation (purple line in Figure 1).

The reanalysis (described in section 2.2) is used to produce a forecast following:

$$\mathbf{x}_k^f = \mathcal{M}(\mathbf{x}_{k-1}^a) \quad (1)$$

where \mathbf{x}_k^f represents the forecasted instantaneous model state at t_k , \mathcal{M} represents the dynamical model integration from time t_{k-1} to t_k (section 2.1). During the analysis, DA uses available observations to generate \mathbf{x}_k^a — an updated instantaneous model state and initial conditions for the next model integration from time t_{k-1} to time t_k .

The online approach is to emulate the analysis increments of DA defined as $\mathbf{x}_k^a - \mathbf{x}_k^f$. The error correction model can be expressed as follows:

$$\varepsilon = \mathcal{M}_e(\mathbf{x}^f) \quad (2)$$



Table 1. Information about online and offline ML-based error correction models

	Online ML-based model	Offline ML-based model
Input features	Instantaneous SST, SSS, latitude, 5 categories SIC and sea ice volume	Monthly SST, SSS, latitude, SIC and sea ice volume
Output features	Instantaneous SST, SSS and 5 categories SIC errors	Monthly SIC prediction error
Data	The most recent eleven years data (ten years for training and one year for validation)	
Remark	Only apply to sea-ice covered grids in the Arctic with SIC values greater than 1%.	

where \mathcal{M}_e represents the data-driven model taking the instantaneous model state \mathbf{x}^f as input and ε represents the estimated
 130 model error. We aim to correct SIC, SST, and SSS errors in the ice-covered area, which are directly associated with the sea ice condition.

Considering the seasonality of the error of the sea ice state, we build one error model (Eq. 2) for each calendar month. Also, we employ a running training strategy and use the most recent 11 years of data before the prediction month (the first 10 years for training and the last year for validation). The input feature contains latitude, SST, SSS, five categories of SIC, and five
 135 categories of sea ice volume in the middle of the month. The output feature consists of errors in SST, SSS, and 5 categories of SIC (Table 1). Please refer to section 2.5 for ML configuration.

The hybrid model incorporating the dynamic model and the online error correction model can be expressed as follows:

$$\mathbf{x}_t^h = \mathcal{M}(\mathbf{x}_{t-1}^h) + \mathcal{M}_e(\mathbf{x}_t^f) \quad (3)$$

where \mathbf{x}_t^h represents the error-corrected instantaneous model state at t_l during the prediction.

140 It is crucial to ensure the physical consistency between the ice and ocean components. Inconsistencies can arise after online error correction, such as through the analysis variables update, which may yield unphysical values, or when certain variables remain uncorrected and must be diagnosed from the updated variables. The post-processing method is specifically designed for NorCPM (Kimmritz et al., 2018).

2.4 Offline error correction approach

145 The offline error correction approach refers to performing post-processing of the dynamical model predictions (blue line in Figure 1). The ML configuration is the same as the online configuration (section 2.5). The input features are monthly SST, SSS, total SIC, and latitude. The output feature is the error in monthly SIC. For more details about the offline approach, please refer to Table 1.



It's worth noting that the offline error correction approach targets directly monthly average model outputs, whereas online
 150 error correction addresses instantaneous model errors (Figure 1) and indirectly changes the monthly model outputs during the
 production of predictions. Therefore, their input and output features are different (Table 1).

2.5 Machine learning configuration

As mentioned in the previous sections, the ML model configurations employed for online and offline error correction ap-
 proaches differ in the input and output variables (for more details, please refer to Table 1), but share an identical architecture
 155 (i.e. the same number of layers and the same number of neurons in each layer).

The ML model uses the values from a single grid point as input to predict the value at the same grid point, meaning one ML
 model for all grid points. This simplifies the training process while still enabling the development of efficient models.

The ML architecture employed in this study is a multilayer perceptron (MLP), a powerful model known for its ability to
 capture complex nonlinear relationships in data. As a fully connected neural network, MLP excels in function approximation,
 160 making it particularly well-suited for error correction in geophysical modeling (Yang et al., 2023). Its key advantages include
 flexibility in handling diverse input features, efficient training through backpropagation, and strong generalization when prop-
 erly regularized. Moreover, MLP is computationally efficient compared to more complex deep learning architectures. As noted
 by Jia et al. (2019) and Watson (2019), error-correcting learning problems generally require smaller ML models and fewer
 training data, making MLP a practical choice for integrating data-driven corrections into NorCPM.

165 The MLP architecture consists of five layers:

- The input layer includes a batch normalization layer (Ioffe, 2017), which helps to regularize and normalize the training
 process.
- The second layer is a dense layer with 60 neurons. It applies the rectified linear unit (ReLU) activation function, which
 introduces non-linearity into the network.
- 170 – The third layer has the same configuration as the second layer, with 30 neurons and ReLU activation function.
- The fourth layer is the attention layer, which is used for helping better training.
- The output layer is a dense layer with a linear activation function.

We further implement the following settings:

- We employ a running training set approach using data from the most recent 11 years. For example, to build an error
 175 correction model for 2021, data from 2010 to 2019 is used for training, and data in 2020 for validation. The primary rea-
 son for using running training is the pronounced decline in Arctic sea ice observed over recent decades, with substantial
 differences between earlier ice conditions (e.g., the 1980s) and those of recent years (e.g., 2010s). We decided to only
 use the data close to the test period. We also performed a sensitivity study on the length of the running training set (e.g.,



the most recent 5 years or all years since 1980), which is not shown in the paper. We found that the data in the most recent 11 years leads to the best performance for ML training.

- The characteristic of model errors varies with the calendar month. For instance, the model errors mainly appear in the marginal zone in winter but in the entire sea ice-covered region in summer. We train separately for each month, leading to a distinct ML model for each month. This results in 236 neural network models (from February 2003 to September 2022 based on test months) for the online case. In the offline case, we consider also the start month, resulting in 836 (4 initialized months \times 11 lead months \times 19 test years) models. Despite the large number of models, the training process is highly efficient due to the simple architecture and low data dimensionality. As a result, training each model is very quick, taking only one minute on a CPU, making this exhaustive approach computationally affordable.
- We train and apply an error correction model to grid points where the total SIC exceeds 1%. It avoids adding sea ice into open water areas and thus dynamical inconsistency. It also means that our correction model can not create ice on a grid point where the model predicted ice-free conditions.

2.6 Hindcast experiments

The standard hindcasts (hereafter referred to as **Reference**) are initialized from the reanalysis presented in section 2.2 in the middle of January, April, July, and October each year, spanning from 1991 to 2021, with a duration of 12 months. From 1991 to 2002, the first 9 ensemble members of the 30-member reanalysis are used to carry out the hindcast experiments, while after 2003, its first 10 ensemble members are used to initialize the hindcast experiments. It is worth noting that these differences (i.e. the number of ensemble members) would have minimal impact on the results of this study.

A new set of hindcasts (hereafter referred to as **OnlineML**), similar to Reference but with the online error correction approach (section 2.3), are initialized from the reanalysis in the middle of January, April, July, and October from 2003 to 2021. In the production of a hindcast, NorCPM pauses in the middle of each lead month and uses the online error correction model (Eq. 2) to predict the error and then update the instantaneous model state.

The offline error correction approach (section 2.4) is applied to post-process the hindcasts of Reference (hereafter referred to as **OfflineML**).

2.7 Metrics for evaluation

SIE is a commonly used metric in seasonal sea ice prediction (e.g., Bushuk et al., 2024). We evaluate the prediction skill of SIE in the Pan-arctic and in six Arctic regions depicted in Fig. 2. These regional delineations adhere to the area definitions provided by Kimmritz et al. (2019), albeit with the consolidation of the original fourteen sea areas into six regions that are very similar to the ones used in Bushuk et al. (2024). In this study, we compute an areal sum of all grid points in the region of interest with $SIC \geq 15\%$ for each ensemble member and evaluate the average of SIEs over different ensemble members.

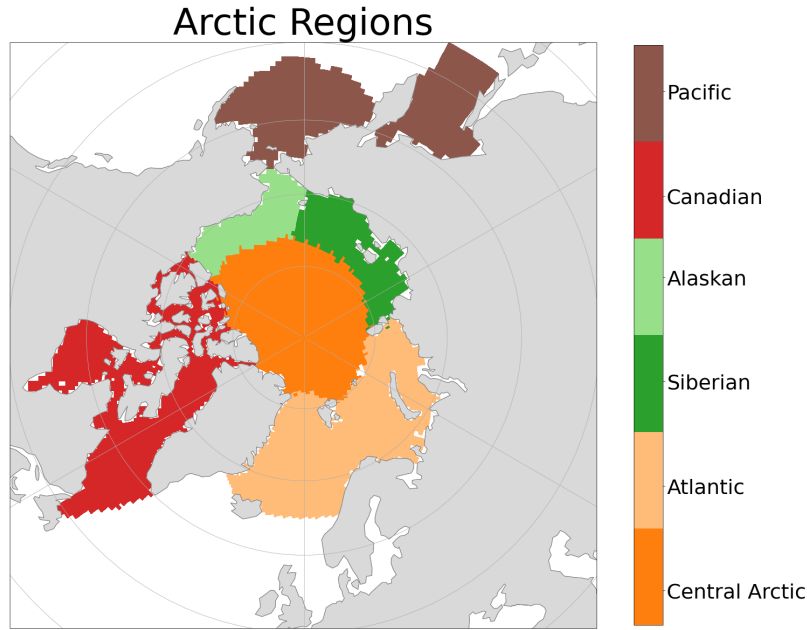


Figure 2. Regional domain definitions for Central Arctic, Atlantic, Siberian, Alaskan, Canadian, and Regions based on sea area definitions in Kimmritz et al. (2019). Atlantic region: GIN Sea, Barents Sea, Kara Sea; Siberian region: Laptev Sea, East Siberian Sea; Alaskan region: Chukchi Sea, Beaufort Sea; Canadian region: Canadian archipelago, Hudson Bay, Baffin Bay, Labrador Sea; Pacific region: Bering Sea, Sea of the Okhotsk.

To evaluate the prediction skill of SIE, we employ the root mean square error (RMSE)

$$210 \quad \text{RMSE} = \sqrt{\frac{1}{N} \sum_{i=1}^N (\mathbf{X}_{\text{prediction}} - \mathbf{X}_{\text{reanalysis}})^2} \quad (4)$$

where $\mathbf{X}_{\text{prediction}}$ represents the prediction and $\mathbf{X}_{\text{reanalysis}}$ represents the reanalysis (i.e., the truth in this study). In this context, \mathbf{X} could refer to either the SIE in the Pan-Arctic/regional scale or the SIC at each grid point. N denotes the length of the experiment period, which spans from 2003 to 2021.

The integrated ice-edge error (IIEE) is also a crucial metric for sea ice predictions (Goessling et al., 2016). It specifically
 215 captures the discrepancies along the ice edge by quantifying the area where the predicted and true ice concentrations differ significantly. This makes IIEE particularly valuable for evaluating the spatial accuracy of the ice edge location, offering insight into the performance of models in reproducing the dynamic boundary between ice-covered and open ocean regions. We define the IIEE as the area where the prediction and the truth disagree on the ice concentration being above or below 15%:

$$\text{IIEE} = \int_A \max(c_p - c_t, 0) dA + \int_A \max(c_t - c_p, 0) dA \quad (5)$$



220 where A is the area of grid cell, $c = 1$ where the sea ice concentration is above 15% and $c = 0$ elsewhere, and subscripts p and t denote the prediction and the truth. The definition of the IIEE is equivalent to the so-called symmetric difference between the areas enclosed by the predicted and true ice edges.

To evaluate the significance of prediction skill, we use a two-tailed Student's t -test to compare IIEE or the squared errors of SIE between two predictions. This statistical test determines whether the difference between the two sets is statistically
 225 significant.

To estimate the uncertainties of the RMSE, we apply the bootstrap method. Specifically, we randomly select, with replacement, 10 data points from the 10 ensemble members, calculate the ensemble mean, and compute the RMSE (either SIC or SIE) for this sampled data. This process is repeated 10,000 times, producing a distribution of 10,000 RMSE values. The standard deviation of this distribution is then used to quantify the uncertainties associated with the RMSE values.

230 3 Results

3.1 Error correction model performance

We first demonstrate the performance of ML-based error correction models in predict the model errors.

The 'true' errors obtained from analysis increments and the errors predicted by the online error correction model are averaged over 2003-2021 and displayed in Fig. 3. The error patterns vary significantly across different dates. For instance, on August
 235 15, the errors are predominantly positive in most regions due to that NorCPM underestimates SIC, with some negative errors occurring internally. On October 15, the errors shift to negative, due to SIC overestimation in NorCPM. On December 15, the errors approach zero, appearing mainly in the marginal areas, with most grid points showing lower error magnitudes compared to August and October. Additionally, the errors along the ice edge remain consistently positive.

For all those months and regions, it shows that the online error correction models can correctly predict the spatial pattern of
 240 the prediction error (Figure 3d-f). The magnitude of the error is well reproduced with a slight underestimation.

To assess the offline error correction model, we show its performance for hindcasts initialized in July (Figure 4). Similar to the instantaneous fields (i.e., online errors in Figure 3), the monthly error patterns vary significantly across months. The offline error correction model effectively predicts the spatial pattern of the prediction errors (Figure 4d-f). The prediction error magnitude is also well captured, with only a slight underestimation.

245 In summary, the above results suggest that the ML error correction models in both online and offline scenarios can skillfully predict the large-scale patterns of the SIC error.

3.2 Application into seasonal predictions

3.2.1 Skill seasonality

In this section, we assess the three sets of hindcasts initialized in January, April, July, and October from 2003 to 2021. The
 250 ensemble hindcasts are initialized with the first 10 members of the reanalyses and predict for 11 months.

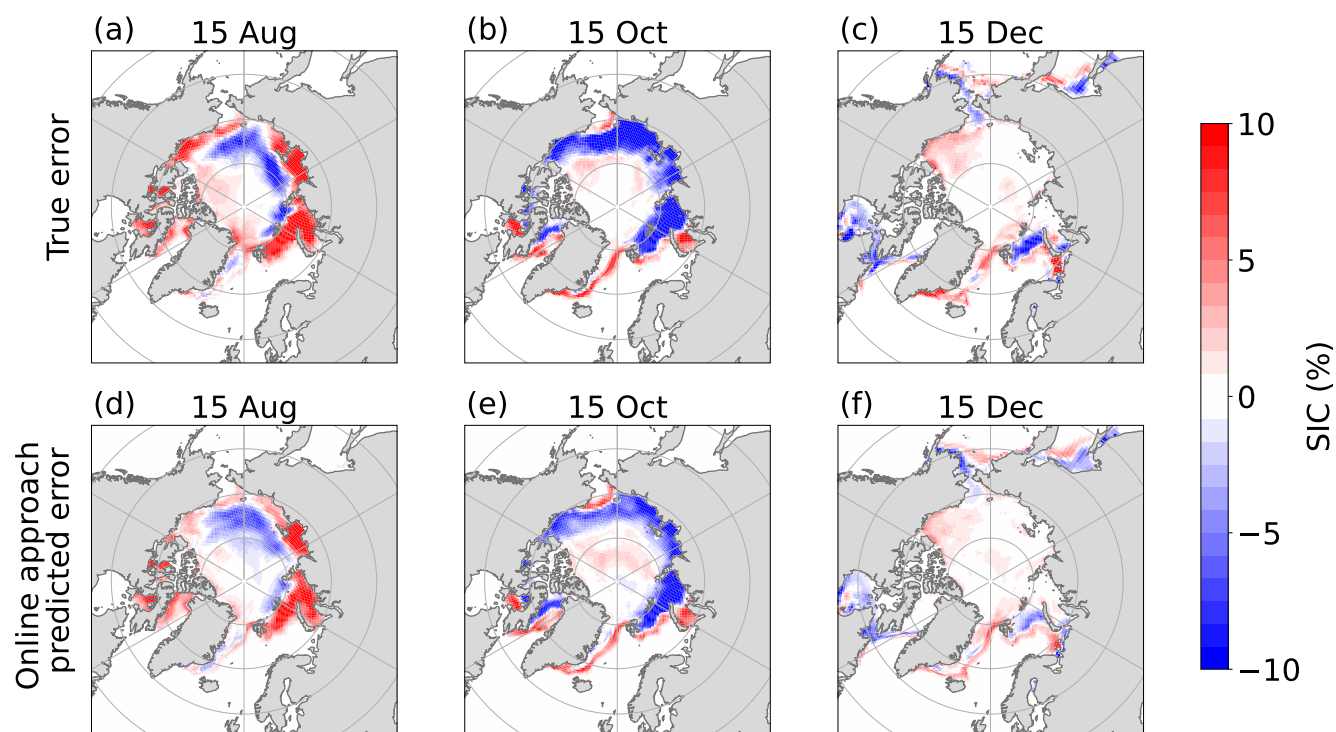


Figure 3. Top row: true errors of SIC in the middle of the month based on the analysis increments. Bottom row: the errors predicted by the online error correction model. These errors are averaged over the period 2003–2021.

Figure 5 presents a comparative analysis of the RMSE for SIE prediction and the IIEE for ice edge prediction in the pan-Arctic across the three hindcast sets. The Reference hindcast shows higher RMSE in September and October (Figure 5a), primarily due to several factors. NorCPM overestimates the Arctic cloudiness and its summer-season snowmelt is too slow. In addition, NorCPM has slightly too weak winds across the polar basin. These factors lead to too thick sea ice in the polar oceans and excessive Arctic SIE, in particular in summer (Bentsen et al., 2013).

Both the OnlineML and OfflineML hindcasts exhibit similar behaviors regardless of the seasonality (Figure 5b and 5c): small error reduction from January to July and a large error reduction from August to December. For OnlineML hindcasts, although only the errors in Arctic SIC, SST, and SSS are corrected without adjusting atmospheric model errors, the predictions show some improvements, particularly in January and from September to December. In contrast, from February to August, the Reference hindcast already exhibits good performance, leading to no significant differences. Compared with the OnlineML hindcasts, the OfflineML hindcasts have a larger error reduction, particularly in September. The primary reason is that the online approach corrects instantaneous model errors (15th day of the month). Still, during the one-month model integration, the sea ice component dynamically interacts with the other components, leading to error growth. In terms of monthly averaged

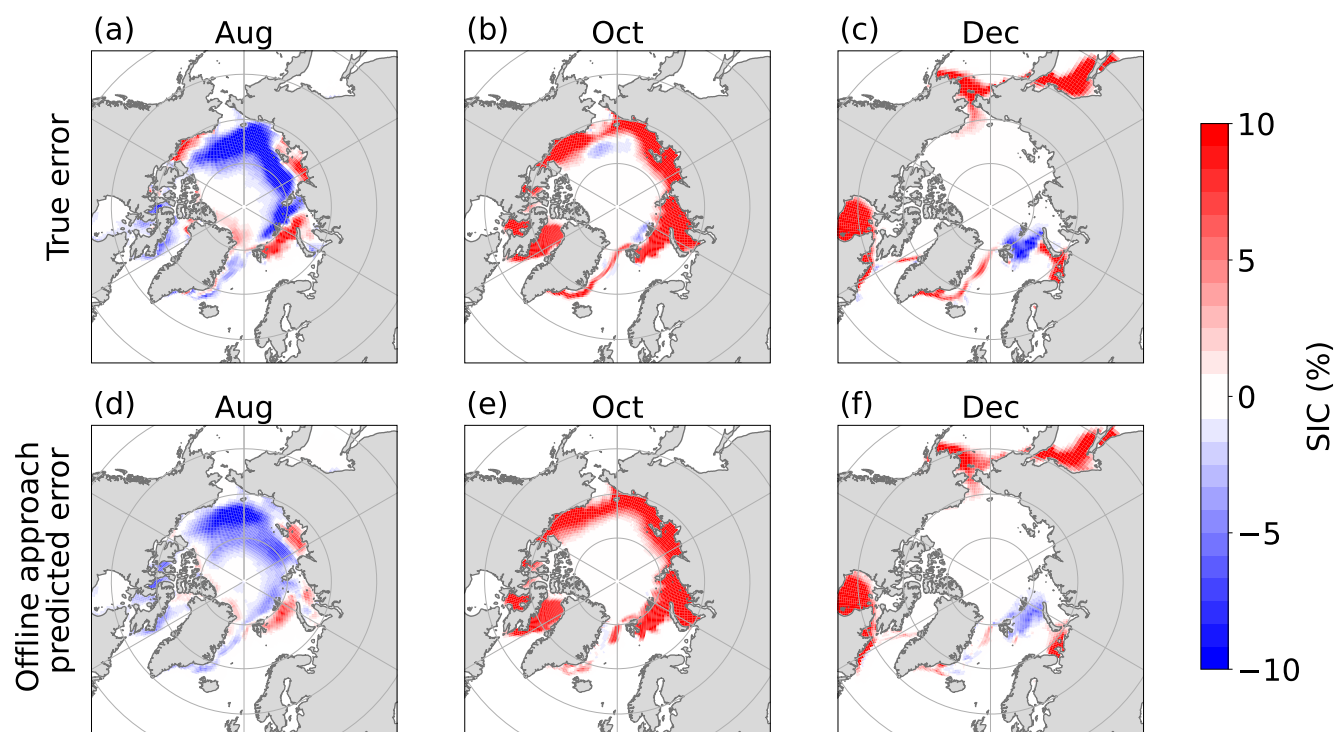


Figure 4. Top row: true errors of monthly SIC estimated by the reanalysis minus the reference hindcast initialized in July. Bottom row: the errors predicted by the offline approach. The errors are averaged over the period 2003–2021.

model outputs, the correction is likely damped. In contrast, the offline approach aims to directly post-process monthly outputs
 265 without model integration.

The IIEE shows similar results to the RMSE of SIE. For the Reference hindcast, the IIEE is higher from July to September. The online approach leads to some improvements over the Reference hindcast from July to December, but its error reduction is small or not significant. In contrast, the offline approach consistently improves the performance across nearly all periods and demonstrates larger error reductions in IIEE than the online approach, particularly from June to January. By directly
 270 correcting monthly mean outputs, the offline approach avoids information loss during the model integration, leading to larger error reduction.

In summary, the Reference hindcast shows larger prediction errors from August to October, due to increased model uncertainties related to atmospheric and sea ice processes. The offline approach outperforms the online approach in reducing both RMSE for SIE and IIEE for ice edge, especially in months with higher prediction errors.

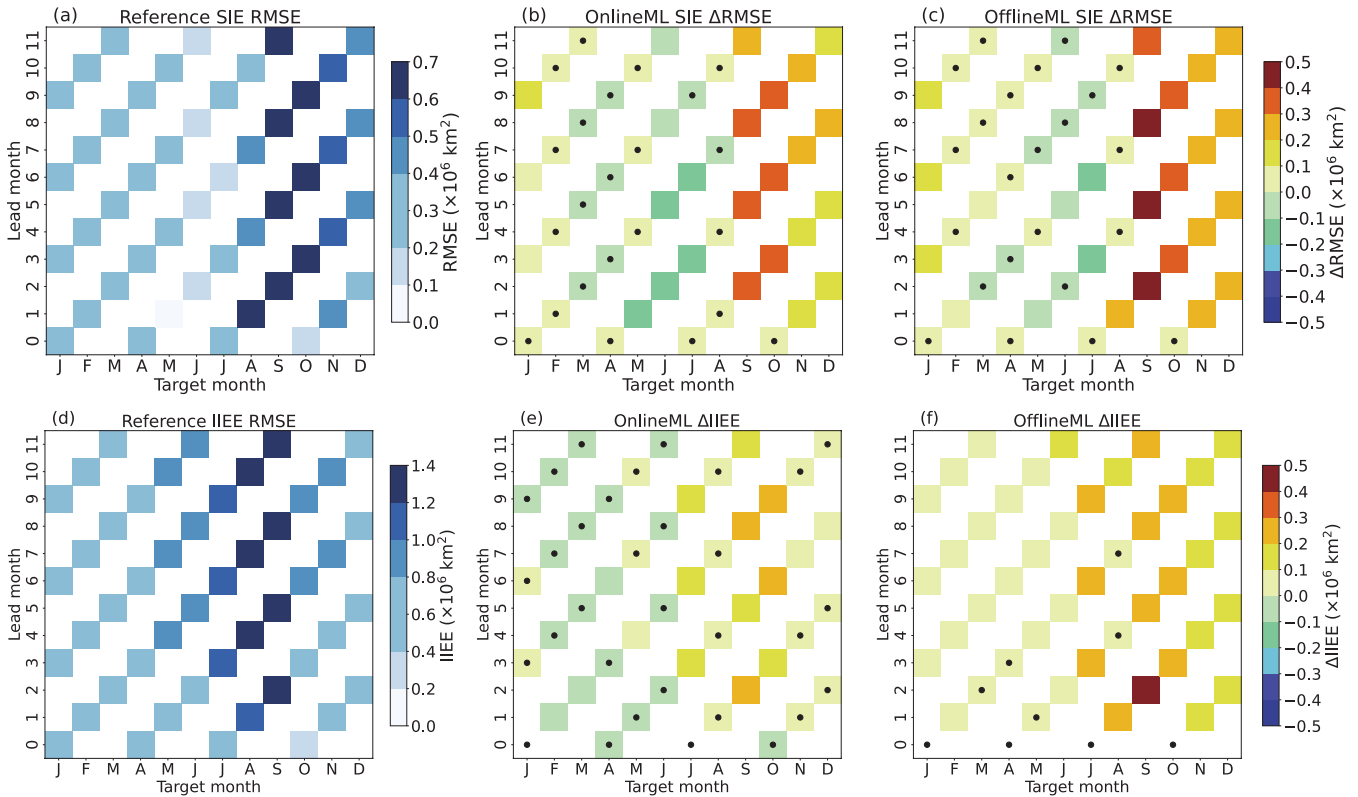


Figure 5. (a) RMSE of SIE for the Reference hindcast, (b) Δ RMSE between the Reference and OnlineML hindcasts, (c) Δ RMSE between the Reference and OfflineML hindcasts. (d) IIEE of the Reference hindcast, (e) Δ IIEE between the Reference and OnlineML hindcasts, (f) Δ IIEE between the Reference and OfflineML hindcasts. In b,c,e, and f, warm colors (red/yellow) indicate that the OnlineML or OfflineML hindcasts are better than the Reference hindcasts, while cold colors (blue/green) indicate they are worse than the Reference hindcast. The black dots represent regions where the Δ RMSE or Δ IIEE does not pass the 95% significance test.

275 3.2.2 Skill of seasonal predictions for different regions

The previous section highlighted significant improvements in predictions, primarily evident from September to January. In this section, we focus on analyzing the hindcasts initialized in July, and we show the performance for different regions and both SIE and SIC. For validation on the other initialization months, please refer to Figures S1-S4.

We first investigate the seasonal prediction skill for pan-Arctic and regional SIE defined in Figure 2. For the pan-Arctic SIE, previously assessed in Fig. 5, both the OnlineML and OfflineML hindcasts reduce the SIE RMSEs (Figure 6a). The RMSEs in the OnlineML hindcast have a strong seasonality as that in the Reference hindcast: higher in August, September, and October, and lower in November, December, and January. The OfflineML hindcast has the lowest RMSEs, in particular, an RMSE reduction of about 70% compared to the Reference hindcasts in September.

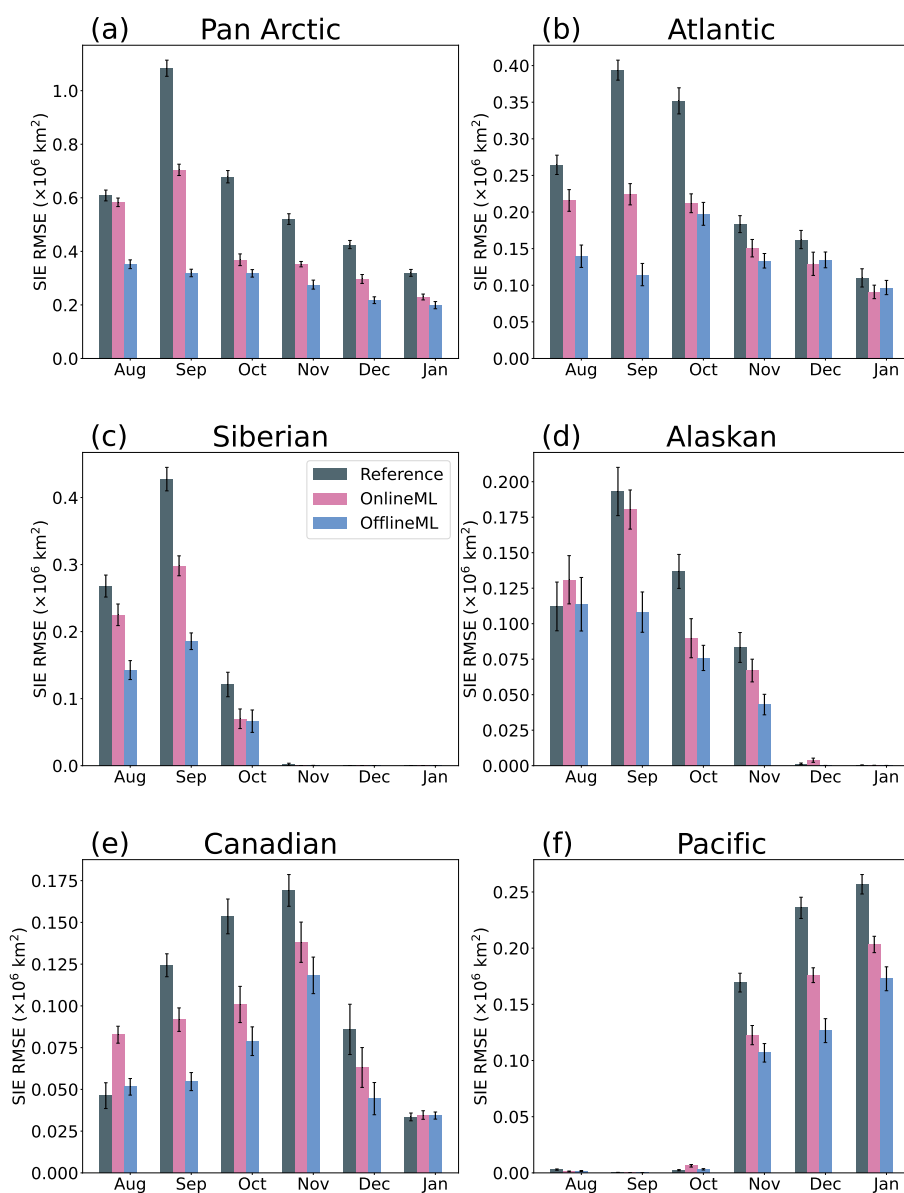


Figure 6. RMSE of SIE in the Pan-Arctic and five subregions for the Reference hindcast (gray bar), the OfflineML hindcast (blue bar), and the OnlineML hindcast (purple bar).



Both error correction approaches reduce the RMSEs for regional SIE, and the offline approach overall outperforms the
 285 online approach (Figure 6b-f). In the Atlantic region (Figure 6b), significant RMSE reduction is observed for the three first
 months, until October. The OfflineML hindcast has the lowest RMSEs until September and similar RMSEs to the OnlineML
 hindcast from October. In the Siberian region (Figure 6c), the RMSE reduction due to error correction is significant only until
 October but becomes almost zeros from November due to the region being fully covered by sea ice. The OfflineML hindcast
 is significantly better than the OnlineML hindcast until September and similar afterwards. In the Alaskan region (Figure 6d),
 290 there is no significant RMSE reduction in August, but we observe significant RMSE reductions from September to November.
 In December and January, the region is almost fully covered by sea ice, leading to very tiny RMSEs for all three hindcast
 experiments. In the Canadian region (Figure 6e), both approaches lead to significant RMSE reductions from September to
 December and the offline approach outperforms the online approach. In addition, the online approach leads to a significantly
 larger RMSE in August than that of the Reference hindcast. In the Pacific region, the RMSEs are near zeros from August to
 295 October due to very limited sea ice coverage. The two error correction approaches lead to significant RMSE reductions after
 November, and the offline approach outperforms the online approach in December and January.

Compared with the online approach, the offline approach performs better in each region. The primary reason is that the
 online approach corrects instantaneous model errors (15th day of the month). The corrected errors may reemerge due to errors
 from other components, damping the error correction when computing monthly averaged model outputs. In contrast, the offline
 300 approach directly corrects the monthly model outputs, which is consistent with the findings for the whole Arctic described in
 the previous section.

In summary, while the error correction performance varies by region and target month, overall, it improves the prediction of
 SIE. In addition, the offline approach is more efficient than the online approach in reducing the SIE RMSEs for both pan-Arctic
 and subregions. For the results of the seasonal predictions initialized in the other seasons, please refer to Figures S1-S4.

305 We take a closer look at the spatial aspects of the offline error correction approach in hindcasts initialized in July (Figure 7).
 We specifically focus on identifying local areas where error correction leads to improvements that may not be evident when
 examining SIE alone.

The improvements in SIC due to error correction are more discernible near the ice edge (Figure 7). In August, only a few grid
 points in the Siberian region and the Atlantic region showed improvements (Figure 7a). In September, significant improvements
 310 are observed, particularly in the central Arctic, Atlantic, Siberian, and Canadian regions (Figure 7b). In October, significant
 enhancements are observed in the Atlantic and Canadian areas. Additionally, some gray areas appear in the central Arctic,
 indicating significant differences between the Reference hindcast and the OfflineML hindcast, though the magnitude of these
 differences is very small. This phenomenon does not occur in the OnlineML hindcast (Figure S5). It suggests that, due to the
 lack of dynamical consistency, OfflineML introduces noises in fully ice-covered regions, but this noise is small. In November
 315 and December, the positive impact of the error correction is concentrated in areas like the Hudson Bay and the Okhotsk Sea.
 In January, the improvements only appear at a few locations within the Okhotsk Sea.

The major improvements in SIC are evident near the ice edge, which is closely associated with SIE. This spatial distribution
 highlights how error correction can enhance model performance in different regions, particularly during the ice-advance season,

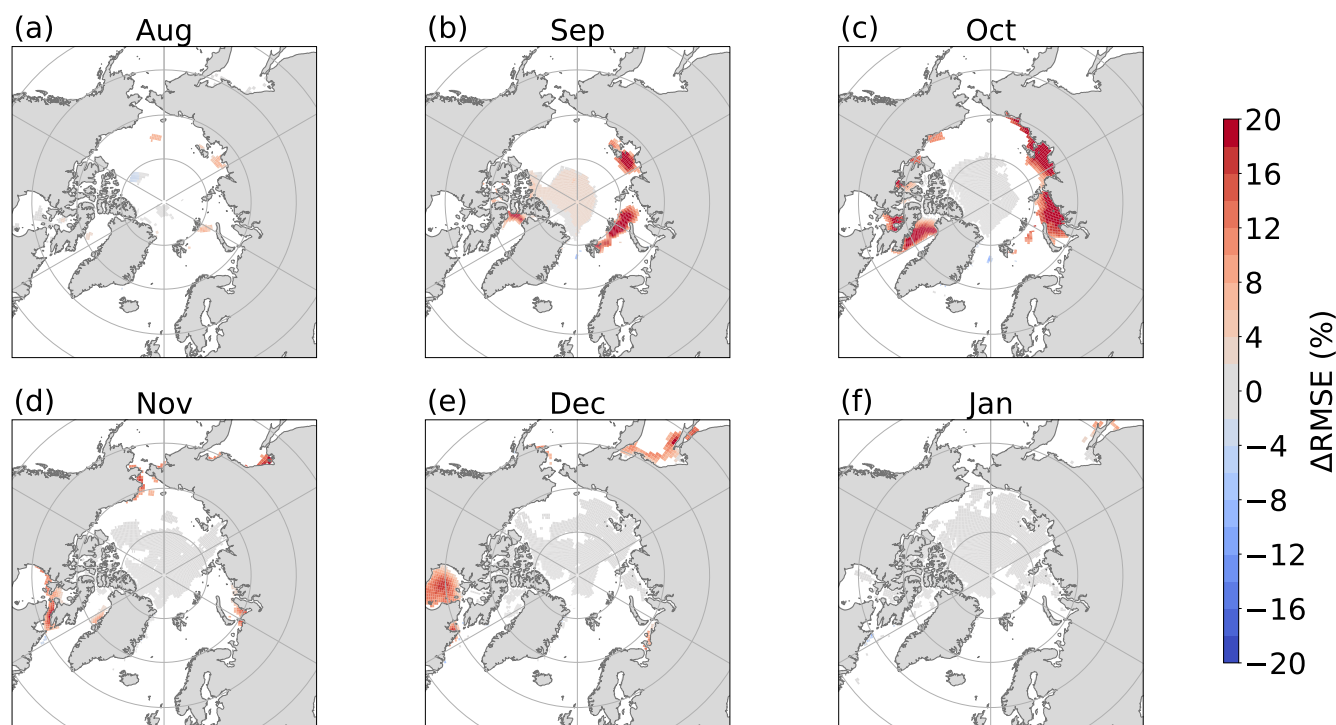


Figure 7. Differences between SIC RMSE of the Reference and OfflineML hindcasts initialized from July. Warmer (colder) colors indicate that the OfflineML hindcast performs better (worse). The white color indicates the differences don't exceed the significant test.

where broader SIE metrics might obscure these localized gains. It is noteworthy that the OfflineML and OnlineML hindcasts
 320 exhibit similar error spatial distributions. For specific details about the OnlineML hindcast, please refer to Figure S5.

4 Discussion and conclusion

In this study, we apply ML in NorCPM – a fully coupled Earth system model – in both online and offline scenarios to improve
 seasonal sea ice predictions in the Arctic. In the context of online error correction, ML is utilized to rectify errors in the middle
 of the month, providing instantaneous corrections that serve as initial conditions for subsequent model integration. The offline
 325 error correction approach involves the post-processing of monthly sea ice predictions.

Our results demonstrate that both the online and offline ML-based error models can well predict the spatial distribution
 of errors, albeit with slight deficiencies in capturing amplitude. By applying the two approaches to seasonal Arctic sea ice
 predictions initialized from January, April, July, and October, we found that both approaches can reduce SIE prediction errors
 compared to the raw predictions without error correction. Moreover, the improvements vary with the lead month, e.g.,
 330 significant improvements from August to October.



Comparing the two error correction approaches, we found that the offline approach overall yields smaller errors than the online approach. This may be because the online approach corrects instantaneous model errors (observed on the 15th day of the month). However, during the model integration, the impact of error correction gradually dissipates due to errors in the other model components. As a result, when computing monthly averaged outputs, the impact of the error correction is damped. It could be beneficial to apply the online error correction model more frequently in time (Gregory et al., 2024). However, the training would not be as straightforward since the analysis increment of NorCPM is only available once per month. Alternatively, training the hybrid model as a whole was beneficial (Farchi et al., 2021) but it requires the external constraint to compute the gradient of the dynamical model, which was not available in our case. In contrast, the offline approach is designed to directly correct the monthly mean output without the need for model integration.

When examining the improvements in regional SIE or SIC, the most significant improvements are observed near the ice edge where sea ice dynamics are active. Overall, the error correction schemes demonstrate their effectiveness in these regions, particularly during the periods when the sea ice dynamics are most pronounced and NorCPM exhibits large errors typically from September to November. During these months, the sea ice margins are subject to rapid changes, and the error correction approaches can capture and adjust for these variations accurately, leading to better model performance in these critical regions.

Our error correction schemes operate on a grid-point basis. As mentioned before, our ML model does not utilize spatial patterns, which explains some of the limitations of our approaches, particularly when the NorCPM's raw hindcasts are already accurate. However, this simplicity offers considerable flexibility in applying the error correction models and reduces the risk of overfitting to specific spatial patterns.

Code and data availability. The code to plot figure is available at <https://doi.org/10.5281/zenodo.14532959>.

Author contributions. Conceptualization: ZH, YW, JB. Analysis and Visualization: ZH. Interpretation of results: ZH, YW, JB. Writing (original draft): ZH, YW. Writing (reviewing and editing original draft): ZH, YW, JB, XW, ZS.

Competing interests. The author declares that no competing interests.

Acknowledgements. This study was funded by the National Key R&D Program of China (2022YFE0106400), the China Scholarship Council (202206710071), Postgraduate Research & Practice Innovation Program of Jiangsu Province (KYCX23_0657), the Special Funds for Creative Research (2022C61540), the Opening Project of the Key Laboratory of Marine Environmental Information Technology (521037412). JB was funded by the project TARDIS funded by the Research Council of Norway grant number 325241. YW was funded by the Norges Forskningsråd (under grant No. 328886) and the Trond Mohn stiftelse (under grant No. BFS2018TMT01). This work also received grants for



computer time from the Norwegian Program for supercomputer (NN9039K) and storage grants (NS9039K). ZS was funded by the National Natural Science Foundation of China (42176003).



360 References

- Bentsen, M., Bethke, I., Debernard, J. B., Iversen, T., Kirkevåg, A., Seland, Ø., Drange, H., Roelandt, C., Seierstad, I. A., Hoose, C., et al.: The Norwegian Earth System Model, NorESM1-M–Part 1: description and basic evaluation of the physical climate, *Geoscientific Model Development*, 6, 687–720, 2013.
- Bethke, I., Wang, Y., Counillon, F., Keenlyside, N., Kimmritz, M., Fransner, F., Samuelsen, A., Langehaug, H., Svendsen, L., Chiu, P.-G.,
 365 et al.: NorCPM1 and its contribution to CMIP6 DCP, *Geoscientific Model Development Discussions*, 2021, 1–84, 2021.
- Blanchard-Wrigglesworth, E., Barthélemy, A., Chevallier, M., Cullather, R., Fučkar, N., Massonnet, F., Posey, P., Wang, W., Zhang, J., Ardilouze, C., et al.: Multi-model seasonal forecast of Arctic sea-ice: forecast uncertainty at pan-Arctic and regional scales, *Climate Dynamics*, 49, 1399–1410, 2017.
- Bleck, R., Dean, S., O’Keefe, M., and Sawdey, A.: A comparison of data-parallel and message-passing versions of the Miami Isopycnic
 370 Coordinate Ocean Model (MICOM), *Parallel computing*, 21, 1695–1720, 1995.
- Blockley, E. W. and Peterson, K. A.: Improving Met Office seasonal predictions of Arctic sea ice using assimilation of CryoSat-2 thickness, *The Cryosphere*, 12, 3419–3438, 2018.
- Brajard, J., Carrassi, A., Bocquet, M., and Bertino, L.: Combining data assimilation and machine learning to infer unresolved scale parametrization, *Philosophical Transactions of the Royal Society A*, 379, 20200086, 2021.
- 375 Bushuk, M., Ali, S., Bailey, D. A., Bao, Q., Batté, L., Bhatt, U. S., Blanchard-Wrigglesworth, E., Blockley, E., Cawley, G., Chi, J., et al.: Predicting September Arctic Sea Ice: A Multi-Model Seasonal Skill Comparison, *Bulletin of the American Meteorological Society*, 2024.
- Carrassi, A., Bocquet, M., Bertino, L., and Evensen, G.: Data assimilation in the geosciences: An overview of methods, issues, and perspectives, *Wiley Interdisciplinary Reviews: Climate Change*, 9, e535, 2018.
- Counillon, F., Bethke, I., Keenlyside, N., Bentsen, M., Bertino, L., and Zheng, F.: Seasonal-to-decadal predictions with the ensemble Kalman
 380 filter and the Norwegian Earth System Model: a twin experiment, *Tellus A: Dynamic Meteorology and Oceanography*, 66, 21 074, 2014.
- Counillon, F., Keenlyside, N., Bethke, I., Wang, Y., Billeau, S., Shen, M. L., and Bentsen, M.: Flow-dependent assimilation of sea surface temperature in isopycnal coordinates with the Norwegian Climate Prediction Model, *Tellus A: Dynamic Meteorology and Oceanography*, 68, 32 437, 2016.
- Craig, A. P., Vertenstein, M., and Jacob, R.: A new flexible coupler for earth system modeling developed for CCSM4 and CESM1, *The
 385 International Journal of High Performance Computing Applications*, 26, 31–42, 2012.
- De Cruz, L., Demaeyer, J., and Vannitsem, S.: The modular arbitrary-order ocean-atmosphere model: MAOOAM v1. 0, *Geoscientific Model Development*, 9, 2793–2808, 2016.
- Dee, D. P., Uppala, S. M., Simmons, A. J., Berrisford, P., Poli, P., Kobayashi, S., Andrae, U., Balmaseda, M., Balsamo, G., Bauer, d. P., et al.: The ERA-Interim reanalysis: Configuration and performance of the data assimilation system, *Quarterly Journal of the royal meteorological
 390 society*, 137, 553–597, 2011.
- Evensen, G.: The ensemble Kalman filter: Theoretical formulation and practical implementation, *Ocean dynamics*, 53, 343–367, 2003.
- Farchi, A., Laloyaux, P., Bonavita, M., and Bocquet, M.: Using machine learning to correct model error in data assimilation and forecast applications, *Quarterly Journal of the Royal Meteorological Society*, 147, 3067–3084, 2021.
- Gent, P. R., Danabasoglu, G., Donner, L. J., Holland, M. M., Hunke, E. C., Jayne, S. R., Lawrence, D. M., Neale, R. B., Rasch, P. J.,
 395 Vertenstein, M., et al.: The community climate system model version 4, *Journal of climate*, 24, 4973–4991, 2011.



- Goessling, H. F., Tietsche, S., Day, J. J., Hawkins, E., and Jung, T.: Predictability of the Arctic sea ice edge, *Geophysical Research Letters*, 43, 1642–1650, <https://doi.org/10.1002/2015GL067232>, 2016.
- Good, S. A., Martin, M. J., and Rayner, N. A.: EN4: Quality controlled ocean temperature and salinity profiles and monthly objective analyses with uncertainty estimates, *Journal of Geophysical Research: Oceans*, 118, 6704–6716, 2013.
- 400 Gregory, W., Bushuk, M., Zhang, Y., Adcroft, A., and Zanna, L.: Machine learning for online sea ice bias correction within global ice-ocean simulations, *Geophysical Research Letters*, 51, e2023GL106776, 2024.
- Hersbach, H., Bell, B., Berrisford, P., Hirahara, S., Horányi, A., Muñoz-Sabater, J., Nicolas, J., Peubey, C., Radu, R., Schepers, D., et al.: The ERA5 global reanalysis, *Quarterly Journal of the Royal Meteorological Society*, 146, 1999–2049, 2020.
- Holland, M. M., Bailey, D. A., Briegleb, B. P., Light, B., and Hunke, E.: Improved sea ice shortwave radiation physics in CCSM4: The
 405 impact of melt ponds and aerosols on Arctic sea ice, *Journal of Climate*, 25, 1413–1430, 2012.
- Ioffe, S.: Batch renormalization: Towards reducing minibatch dependence in batch-normalized models, *Advances in neural information processing systems*, 30, 2017.
- Jia, X., Willard, J., Karpatne, A., Read, J., Zwart, J., Steinbach, M., and Kumar, V.: Physics guided RNNs for modeling dynamical systems: A case study in simulating lake temperature profiles, in: *Proceedings of the 2019 SIAM international conference on data mining*, pp. 558–566, SIAM, 2019.
- 410 Jung, T., Gordon, N. D., Bauer, P., Bromwich, D. H., Chevallier, M., Day, J. J., Dawson, J., Doblas-Reyes, F., Fairall, C., Goessling, H. F., et al.: Advancing polar prediction capabilities on daily to seasonal time scales, *Bulletin of the American Meteorological Society*, 97, 1631–1647, 2016.
- Kimmritz, M., Counillon, F., Bitz, C., Massonnet, F., Bethke, I., and Gao, Y.: Optimising assimilation of sea ice concentration in an Earth
 415 system model with a multicategory sea ice model, *Tellus A: Dynamic Meteorology and Oceanography*, 70, 1–23, 2018.
- Kimmritz, M., Counillon, F., Smedsrud, L. H., Bethke, I., Keenlyside, N., Ogawa, F., and Wang, Y.: Impact of ocean and sea ice initialisation on seasonal prediction skill in the Arctic, *Journal of Advances in Modeling Earth Systems*, 11, 4147–4166, 2019.
- Kirkevåg, A., Grini, A., Olivié, D., Seland, Ø., Alterskjær, K., Hummel, M., Karset, I. H., Lewinschal, A., Liu, X., Makkonen, R., et al.: A production-tagged aerosol module for Earth system models, OsloAero5. 3–extensions and updates for CAM5. 3–Oslo, *Geoscientific
 420 Model Development*, 11, 3945–3982, 2018.
- Laloyaux, P., de Boisseson, E., Balmaseda, M., Bidlot, J.-R., Broennimann, S., Buizza, R., Dalhgren, P., Dee, D., Haimberger, L., Hersbach, H., et al.: CERA-20C: A coupled reanalysis of the twentieth century, *Journal of Advances in Modeling Earth Systems*, 10, 1172–1195, 2018.
- Lawrence, D. M., Oleson, K. W., Flanner, M. G., Thornton, P. E., Swenson, S. C., Lawrence, P. J., Zeng, X., Yang, Z.-L., Levis, S., Sakaguchi, K., et al.: Parameterization improvements and functional and structural advances in version 4 of the Community Land Model, *Journal of
 425 Advances in Modeling Earth Systems*, 3, 2011.
- Palermé, C., Lavergne, T., Rusin, J., Melsom, A., Brajard, J., Kvanum, A. F., Macdonald Sørensen, A., Bertino, L., and Müller, M.: Improving short-term sea ice concentration forecasts using deep learning, *The Cryosphere*, 18, 2161–2176, 2024.
- Penny, S. G. and Hamill, T. M.: Coupled data assimilation for integrated earth system analysis and prediction, *Bulletin of the American
 430 Meteorological Society*, 98, ES169–ES172, 2017.
- Reynolds, R. W., Smith, T. M., Liu, C., Chelton, D. B., Casey, K. S., and Schlax, M. G.: Daily high-resolution-blended analyses for sea surface temperature, *Journal of climate*, 20, 5473–5496, 2007.



- Saha, S., Nadiga, S., Thiaw, C., Wang, J., Wang, W., Zhang, Q., Van den Dool, H., Pan, H.-L., Moorthi, S., Behringer, D., et al.: The NCEP climate forecast system, *Journal of Climate*, 19, 3483–3517, 2006.
- 435 Serreze, M. C., Holland, M. M., and Stroeve, J.: Perspectives on the Arctic’s shrinking sea-ice cover, *science*, 315, 1533–1536, 2007.
- Stroeve, J. C., Markus, T., Boisvert, L., Miller, J., and Barrett, A.: Changes in Arctic melt season and implications for sea ice loss, *Geophysical Research Letters*, 41, 1216–1225, 2014.
- Taylor, K. E., Stouffer, R. J., and Meehl, G. A.: An overview of CMIP5 and the experiment design, *Bulletin of the American meteorological Society*, 93, 485–498, 2012.
- 440 Thornton, E.: Technical Description of version 4.0 of the Community Land Model (CLM), NCAR, Climate and Global, 2010.
- Titchner, H. A. and Rayner, N. A.: The Met Office Hadley Centre sea ice and sea surface temperature data set, version 2: 1. Sea ice concentrations, *Journal of Geophysical Research: Atmospheres*, 119, 2864–2889, 2014.
- Vitart, F., Ardilouze, C., Bonet, A., Brookshaw, A., Chen, M., Codorean, C., Déqué, M., Ferranti, L., Fucile, E., Fuentes, M., Hendon, H., Hodgson, J., Kang, H.-S., Kumar, A., Lin, H., Liu, G., Liu, X., Malguzzi, P., Mallas, I., Manoussakis, M., Mastrangelo, D., MacLachlan, C.,
- 445 McLean, P., Minami, A., Mladek, R., Nakazawa, T., Najm, S., Nie, Y., Rixen, M., Robertson, A. W., Ruti, P., Sun, C., Takaya, Y., Tolstykh, M., Venuti, F., Waliser, D., Woolnough, S., Wu, T., Won, D.-J., Xiao, H., Zaripov, R., and Zhang, L.: The Subseasonal to Seasonal (S2S) Prediction Project Database, *Bulletin of the American Meteorological Society*, 98, 163 – 173, <https://doi.org/10.1175/BAMS-D-16-0017.1>, 2017.
- Wagner, P. M., Hughes, N., Bourbonnais, P., Stroeve, J., Rabenstein, L., Bhatt, U., Little, J., Wiggins, H., and Fleming, A.: Sea-ice information and forecast needs for industry maritime stakeholders, *Polar Geography*, 43, 160–187, 2020.
- 450 Wang, W., Chen, M., and Kumar, A.: Seasonal prediction of Arctic sea ice extent from a coupled dynamical forecast system, *Monthly Weather Review*, 141, 1375–1394, 2013.
- Wang, Y., Counillon, F., and Bertino, L.: Alleviating the bias induced by the linear analysis update with an isopycnal ocean model, *Quarterly Journal of the Royal Meteorological Society*, 142, 1064–1074, 2016.
- 455 Wang, Y., Counillon, F., Bethke, I., Keenlyside, N., Bocquet, M., and Shen, M.-l.: Optimising assimilation of hydrographic profiles into isopycnal ocean models with ensemble data assimilation, *Ocean Modelling*, 114, 33–44, 2017.
- Wang, Y., Counillon, F., Keenlyside, N., Svendsen, L., Gleixner, S., Kimmritz, M., Dai, P., and Gao, Y.: Seasonal predictions initialised by assimilating sea surface temperature observations with the EnKF, *Climate Dynamics*, 53, 5777–5797, 2019.
- Watson, P. A.: Applying machine learning to improve simulations of a chaotic dynamical system using empirical error correction, *Journal of*
- 460 *Advances in Modeling Earth Systems*, 11, 1402–1417, 2019.
- Watt-Meyer, O., Brenowitz, N. D., Clark, S. K., Henn, B., Kwa, A., McGibbon, J., Perkins, W. A., and Bretherton, C. S.: Correcting weather and climate models by machine learning nudged historical simulations, *Geophysical Research Letters*, 48, e2021GL092555, 2021.
- Yang, Z., Liu, J., Yang, C.-Y., and Hu, Y.: Correcting nonstationary sea surface temperature bias in NCEP CFSv2 using Ensemble-based Neural Networks, *Journal of Atmospheric and Oceanic Technology*, 40, 885–896, 2023.
- 465 Zuo, H., Balmaseda, M. A., Tietsche, S., Mogensen, K., and Mayer, M.: The ECMWF operational ensemble reanalysis–analysis system for ocean and sea ice: a description of the system and assessment, *Ocean science*, 15, 779–808, 2019.